THE JOURNAL OF BIOLOGICAL CHEMISTRY VOL. 288, NO. 8, pp. 5487–5495, February 22, 2013

Gating Transitions in the Palm Domain of ASIC1a*

Received for publication, December 3, 2012, and in revised form, January 2, 2013 Published, JBC Papers in Press, January 8, 2013, DOI 10.1074/jbc.M112.441964

Margaret C. Della Vecchia[‡], Anna C. Rued[‡], and Marcelo D. Carattino[‡§1]

From the [‡]Renal-Electrolyte Division, Department of Medicine, and the [§]Department of Cell Biology, University of Pittsburgh, Pittsburgh, Pennsylvania 15261

Background: Extracellular acidification promotes structural rearrangements in the ectodomain of ASIC1a that result in activation and desensitization.
Results: Glu-79 and Glu-416 cooperatively facilitate proton gating. The lower palm domain contracts upon extracellular acidification.
Conclusion: The lower palm domain mediates conformational changes that drive pore opening and closing events.
Significance: This study provides insight into the molecular mechanism of gating of epithelial sodium/degenerin channels.

Acid-sensing ion channels (ASICs) are trimeric cation-selective proton-gated ion channels expressed in the central and peripheral nervous systems. The pore-forming transmembrane helices in these channels are linked by short loops to the palm domain in the extracellular region. Here, we explore the contribution to proton gating and desensitization of Glu-79 and Glu-416 in the palm domain of ASIC1a. Engineered Cys, Lys, and Gln substitutions at these positions shifted apparent proton affinity toward more acidic values. Double mutant cycle analysis indicated that Glu-79 and Glu-416 cooperatively facilitated pore opening in response to extracellular acidification. Channels bearing Cys at position 79 or 416 were irreversibly modified by thiol-reactive reagents in a state-dependent manner. Glu-79 and Glu-416 are located in β-strands 1 and 12, respectively. The covalent modification by (2-(trimethylammonium)ethyl) methanethiosulfonate bromide of Cys at position 79 impacted conformational changes associated with pore closing during desensitization, whereas the modification of Cys at position 416 affected conformational changes associated with proton gating. These results suggest that β-strands 1 and 12 contribute antagonistically to activation and desensitization of ASIC1a. Site-directed mutagenesis experiments indicated that the lower palm domain contracts in response to extracellular acidification. Taken together, our studies suggest that the lower palm domain mediates conformational movements that drive pore opening and closing events.

Acid-sensing ion channels (ASICs)[2] are neuronal cation-selective proton-gated channels that contribute to nociception, mechanosensation, synaptic plasticity, learning and memory, and fear conditioning (1–6). ASICs belong to the epithelial sodium channel/degenerin family of ion channels, a group of proteins that share a similar overall organization with two transmembrane helices (TMs) connected by a large extracellular region with intracellular N and C termini. Four genes encoding ASIC subunits and their splice variants (ASIC1–4) have been identified in mammals (4, 7, 8). ASIC subunits assemble to form homo- or heterotrimers, which have functional properties that resemble those of proton-gated channels in neurons (4, 8–10). At neutral pH, ASICs reside in a closed or resting state and transition to an open conductive state upon extracellular acidification. The residency time in the open state and the proton apparent affinity depend on the subunits forming the channel complex (9, 11). After the initial drop in extracellular pH, ASICs desensitize and become unresponsive to extracellular protons. The transition from the desensitized state to the closed state requires deprotonation of one or more groups and occurs upon return to high pH.

The molecular mechanisms that promote pore opening and closing events on ASICs are not well defined. Titratable residues in the extracellular region have been considered as potential sites for proton binding on these channels. The extracellular region of chicken ASIC1 (cASIC1) encompasses discrete domains referred to as the thumb, finger, palm, β-ball, and knuckle (12). TM1 and TM2 are connected by short loops to the β-strands 1 and 12 in the lower palm domain, respectively. Inspection of the electrostatic potential mapped onto the solvent-accessible surface of cASIC1 revealed a highly negatively charged cavity in the extracellular region (12). This acidic pocket was proposed to serve as the primary site for proton sensing. Although mutations introduced at certain positions within the pocket altered apparent proton affinity, these channels remained proton-sensitive, suggesting that additional residues serve as proton-binding sites (12–14). Recently, Liechti *et al.* (15) combined computational and functional approaches to identify additional acidic residues that contribute to proton gating in the extracellular region of ASIC1a. Overall, these functional studies indicate that residues distributed throughout the extracellular domain contribute to proton gating.

We recently reported that the loop preceding TM2 in ASIC1a reorganizes in tandem with pore opening (16). Similarly, the short segments preceding TM1 and TM2 modulate the epithelial sodium channel's response to external factors

* This work was supported, in whole or in part, by National Institutes of Health Grant R01 DK084060.
[1] To whom correspondence should be addressed: Renal-Electrolyte Div., Dept. of Medicine, S828 Scaife Hall, 3550 Terrace St., Pittsburgh, PA 15261. Tel.: 412-624-5437; E-mail: mdc4@pitt.edu.
[2] The abbreviations used are: ASIC, acid-sensing ion channel; TM, transmembrane helix; cASIC1, chicken ASIC1; MTS, methanethiosulfonate; MTSET, (2-(trimethylammonium)ethyl) methanethiosulfonate bromide; MTSMT, (1-(trimethylammonium)methyl) methanethiosulfonate bromide; MTSPT, (3-(trimethylammonium)propyl) methanethiosulfonate bromide; GMQ, 2-guanidine-4-methylquinazoline.

(17). These studies suggest that the transmembrane-extracellular region junction experiences significant structural changes during channel gating. In agreement with these studies, psalmotoxin-ASIC complexes in an apparently permeable conformation illustrate an expansion of the conductive pathway concomitantly with a contraction of the extracellular vestibule in the lower palm domain (18). Although structural information on cASIC1 in the closed state is not currently available, these studies suggest that the lower palm domain experiences an important rearrangement in response to extracellular acidification.

Here, we investigated the contribution to ASIC1a gating and desensitization of two acidic residues in the palm domain, Glu-79 and Glu-416. These residues form a hexagon-like structure in the extracellular vestibule in the desensitized-like state (12, 19). Site-directed mutagenesis studies revealed that functional coupling between Glu-79 and Glu-416 facilitates pore opening in response to extracellular acidification. To define conformational changes in the lower palm domain that occur in response to extracellular acidification, we conducted studies of accessibility with thiol-reactive reagents on channels bearing Cys at positions 79 and 416. The results of these studies indicate that the palm domain of ASIC1a resides in an expanded conformation at resting pH and transitions to a contracted conformation following extracellular acidification.

EXPERIMENTAL PROCEDURES

Reagents—Methanethiosulfonate (MTS) reagents were from Toronto Research Chemicals (North York, Ontario, Canada). All other reagents were from Sigma-Aldrich.

Molecular Biology and Oocyte Expression—Mutations were generated in a mouse ASIC1a construct carrying a Leu mutation at position 70 and a C-terminal hemagglutinin epitope tag. We previously showed that the modification by thiol-reactive reagents of Cys-70 in wild-type mouse ASIC1a reduces proton-gated currents (16). Site-directed mutagenesis was performed with a QuikChange XL kit (Agilent Technologies, Santa Clara, CA) according to the manufacturer's instructions. Mutations were confirmed by direct sequencing. Constructs were transcribed using a mMESSAGE mMachine SP6 kit (Applied Biosystems). Oocytes at stages 5–6 were harvested from adult female *Xenopus laevis* (Nasco, Salida, CA) according to a protocol approved by the University of Pittsburgh Institutional Animal Care and Use Committee. Oocytes were injected with 0.05–6 ng of cRNA encoding ASIC1a mutants and maintained at 18 °C in modified Barth's solution containing 88 mM NaCl, 1 mM KCl, 2.4 mM $NaHCO_3$, 15 mM HEPES, 0.3 mM $Ca(NO_3)_2$, 0.41 mM $CaCl_2$, 0.82 mM $MgSO_4$, 10 μg/ml sodium penicillin, 10 μg/ml streptomycin sulfate, and 100 μg/ml gentamycin sulfate (pH 7.4).

Electrophysiology—Experiments were conducted 24–48 h after injection at room temperature (20–25 °C). Oocytes were placed in a recording chamber with a volume of ~20 μl (Auto-Mate Scientific, Berkeley, CA) and impaled with glass electrodes filled with 3 M KCl. The resistance of the glass electrodes was 0.2–2 megohms. Two-electrode voltage clamp experiments were conducted with a TEV-200A amplifier (Dagan Corp., Minneapolis, MN). Data were captured with a Digidata 1440A acquisition system and analyzed with pCLAMP 10 (Molecular Devices, Sunnyvale, CA). Oocytes were continuously clamped at a holding potential of −60 mV. The recording solution contained 110 mM NaCl, 2 mM KCl, 1 mM $CaCl_2$, and 10 mM HEPES. Acidic test solutions were buffered with MES.

Modification of Cys Residues—Oocytes expressing ASIC1a channels with Cys mutations were mounted in the recording chamber as described above. MTS reagents were dissolved in the recording solution before the experiments to a final concentration of 1 mM. Solutions containing MTS reagents buffered at pH 8.0, 7.6, 7.4, or 7.2 were used immediately, whereas solutions buffered at pH 7.0 were used within 30 min of preparation. The half-time of hydrolysis for (2-(trimethylammonium)ethyl) methanethiosulfonate bromide (MTSET) at pH 7.0 is 130 min (20). ASIC1a mutants were treated with MTS reagents at pH 8.0, *i.e.* channels in the closed state, or at pH 7.0, *i.e.* channels in the desensitized state.

Data and Statistical Analysis—Data are expressed as the mean ± S.E. (n), where n indicates the number of independent experiments analyzed. Data were collected from a minimum of two batches of oocytes. A p value of <0.05 was considered statistically significant. For statistical analyses, the normality and equality of the standard deviation of the data were tested. Based on these results, a parametric or a nonparametric test was used. The pH of half-maximal activation (pH_{50}) was calculated from normalized currents plotted as a function of the extracellular pH and fitted with Equation 1,

$$I = I_{min} + (I_{max} - I_{min})/(1 + 10^{(pH_{50} - X)}) \quad \text{(Eq. 1)}$$

where I is the macroscopic current, X is the extracellular pH, and pH_{50} is the extracellular pH that provokes a response halfway between the base-line (I_{min}) and maximum (I_{max}) response. The fractional activation represents the ratio of the peak current elicited by a change of pH from 9.0 to a solution of lower pH to the peak current evoked by a drop from pH 9.0 to 4.0. The pH of half-maximal steady-state desensitization (pH_d) was estimated from normalized currents plotted as a function of the extracellular pH and fitted with Equation 2,

$$I = I_{min} + (I_{max} - I_{min})/(1 + 10^{(pH_d - X)n}) \quad \text{(Eq. 2)}$$

where n is the Hill coefficient, and pH_d is the preconditioning pH that produces a response half-way between the base-line and maximum response. pH_{50} and pH_d are expressed as the mean ± S.E. with a 95% confidence interval. ASIC1a tachyphylaxis refers to a decrease in the magnitude of the proton-gated currents observed after consecutive stimulation (21). To minimize the impact of tachyphylaxis in the determination of pH_{50} and pH_d, channels were subject to only three cycles of activation. The time constants of desensitization were estimated by fitting experimental data to a single exponential function, $I = I_0 \cdot \exp^{-t/\tau} + c$, where I is the macroscopic current, τ is the time constant of desensitization, and c and I_0 are constants determined by curve fitting. Fitting and statistical comparisons were performed with Clampfit (Molecular Devices), SigmaPlot 11.0 (Systat Software, Chicago, IL), and GraphPad 5.03 (GraphPad Software, San Diego, CA).

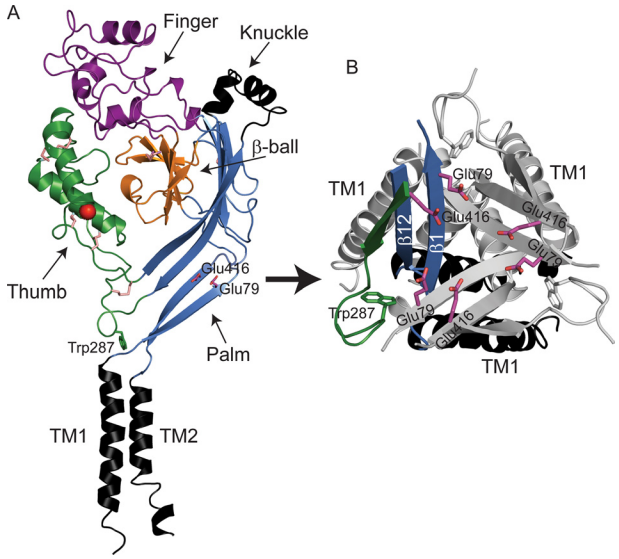

FIGURE 1. **Structural model of ASIC1 illustrating the locations of Glu-79 and Glu-416.** *A*, schematic representation of a cASIC1 subunit in the desensitized state. Glu-79 and Glu-416 in the palm domain are shown (Protein Data Bank code 3HGC). The chloride ion is shown as a *red ball*, and disulfide bridges are shown as *pink sticks*. cASIC1 and mouse ASIC1a share 89.6% amino acid identity. Residue numbering corresponds to mouse ASIC1a. *B*, close-up view of Glu-79 and Glu-416 in the palm domain.

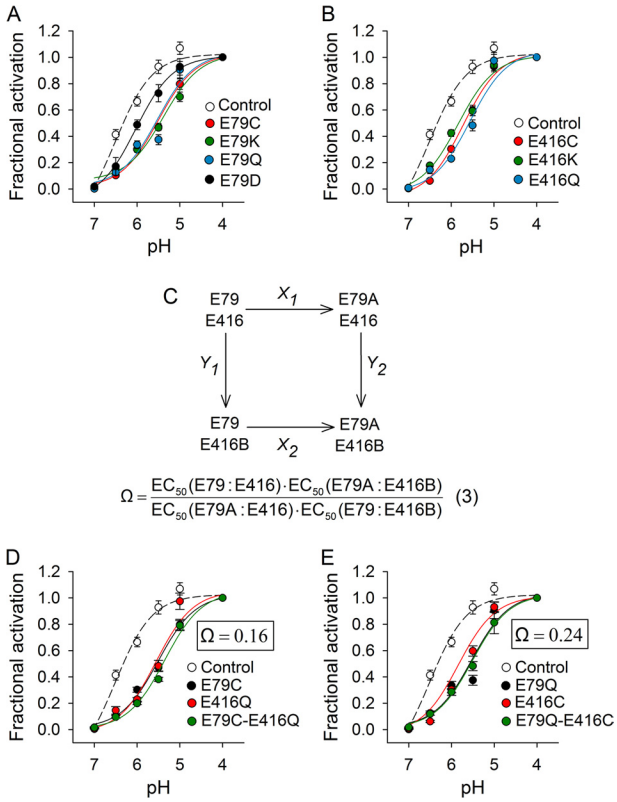

$$\Omega = \frac{EC_{50}(E79:E416)\cdot EC_{50}(E79A:E416B)}{EC_{50}(E79A:E416)\cdot EC_{50}(E79:E416B)} \quad (3)$$

FIGURE 2. **Functional coupling of Glu-79 and Glu-416.** *A* and *B*, proton activation curves for control (C70L) and mutant channels. Proton-activated currents were elicited by a drop in extracellular pH from 9.0 to solutions of lower pH. Currents were normalized to the signal obtained at pH 4.0 (n = 8–30). *C*, double mutant cycle for Glu-79 and Glu-416. Shown is the apparent proton affinity (EC_{50}) for the control channel (*E79:E416*) and the single (*E79A:E416* and *E79:E416B*) and double (*E79A:E416B*) mutant channels. *D* and *E*, proton activation curves for control, single, and double mutant channels. Proton-activated currents were elicited by a drop in extracellular pH from 9.0 to solutions of lower pH. Currents were normalized to the signal obtained at pH 4.0 (n = 9–28). The coupling coefficient (Ω) was calculated according to Equation 3 for double mutant cycles.

RESULTS

Glu-79 and Glu-416 Contribute to Proton Gating—Here, we explored the contribution to channel activation and desensitization of Glu-79 and Glu-416 (Fig. 1). Glu-79 is conserved within ASIC subunits that generate proton-gated currents as homomers, whereas Glu-416 is present in virtually all ASIC isoforms. In the desensitized state, Glu-79 and Glu-416 are hexagonally arranged in the lower palm domain (Protein Data Bank code 3HGC) (Fig. 1). The distance between Glu-79 and Glu-416 within the same subunit is 4.4 Å, whereas the distance between these residues in neighboring subunits is 5.7 Å. Because these two acidic residues are relatively close in space, Jasti *et al.* (12) proposed that at least one of the carboxyl groups is protonated at low pH. To determine the contribution of Glu-79 and Glu-416 to activation and desensitization, we first individually mutated these residues to Cys, Lys, and Gln (Fig. 2). These mutations shifted the apparent proton affinity for activation toward more acidic values (Fig. 2 and Table 1). Some mutations at these positions shifted the apparent proton affinity for steady-state desensitization slightly toward more alkaline values (Table 1). Cys, Lys, and Gln substitutions at positions 79 and 416 produced a similar shift in pH_{50} toward more acidic values. An Asp substitution at position 79 generated only a modest change in pH_{50} by comparison (Fig. 2 and Table 1). Channels bearing mutations at position 79 desensitized faster than controls (Table 1), which is consistent with previous studies conducted with ASIC3 (22). These results suggest that negatively charged residues at positions 79 and 416 facilitate pore opening in response to extracellular acidification.

Glu-79 and Glu-416 Are Functionally Coupled—Individual Cys, Lys, and Gln mutations at position 79 or 416 shifted pH_{50} toward more acidic values to a similar extent, suggesting a functional coupling between Glu-79 and Glu-416. To assess energetic coupling between Glu-79 and Glu-416, we conducted double mutant cycle analysis (23, 24). The coupling coefficient, Ω, is defined as in Equation 3,

$$\Omega = \frac{EC_{50}(\text{Glu-79/Glu-416}) \cdot EC_{50}(\text{E79}A\text{/E416}B)}{EC_{50}(\text{E79}A\text{/Glu-416}) \cdot EC_{50}(\text{Glu-79/E416}B)} \quad \text{(Eq. 3)}$$

where *A* and *B* represent mutations at positions 79 and 416, respectively. If the mutated amino acids are not functionally coupled, then Ω will be unity. If the residues are functionally coupled and the mutations alter their interaction, then Ω will deviate from unity. We generated two double mutant constructs (E79C/E416Q and E79Q/E416C) and measured the pH_{50} (Fig. 2, *D* and *E*). The calculated coupling coefficient (Ω) for the sets E79C/E416Q and E79Q/E416C were 0.16 and 0.24, respectively. These results demonstrate that Glu-79 and Glu-416 cooperatively facilitate pore opening.

Reactivity toward MTS Reagents of Cys at Positions 79 and 416 Is State-dependent—Glu-79 and Glu-416 are situated within the core of the palm domain in β1 and β12, respectively (Fig. 1). These β-strands are directly linked to the TMs by short loops. We previously showed that the region that connects TM2 to β12 rearranges following extracellular acidification and

TABLE 1

Biochemical characterization of ASIC1a mutants

For pH dependence of activation, proton-activated currents were elicited by a drop in extracellular pH from 9.0 to solutions of lower pH. Currents were normalized to the signal obtained at pH 4.0. pH_{50} is the log of the concentration of protons yielding a current at half-maximum ($n = 8–30$). For pH dependence of desensitization, whole-cell currents were elicited by extracellular acidification to pH 5.0 from a solution of pH 9.0, 8.0, 7.8, 7.6, 7.4, 7.2, or 7.0. Currents were normalized to the signal obtained at pH 9.0. pH_d is the log of the concentration of protons in the preconditioning solution yielding a current at half-maximum, and n is the Hill coefficient estimated for desensitization ($n = 9–11$). pH_{50} and pH_d are expressed as the mean ± S.E. with a 95% confidence interval (CI). The time constants of desensitization (τ_d) were estimated by fitting experimental data to a single exponential function as described under "Experimental Procedures" ($n = 9–26$). Proton-activated currents were elicited by a drop in extracellular pH from 9.0 to 5.0. ND, not determined.

Mutant	pH_{50}	CI pH_{50}	pH_d	CI pH_d	n	τ_d
						s
C70L	6.51 ± 0.07	6.37–6.56	7.39 ± 0.02	7.35–7.42	11.3	1.56 ± 0.17
E79C	5.51 ± 0.04	5.42–5.59	7.51 ± 0.02	7.47–7.52	8.3	0.60 ± 0.04
E79C + MTSET	5.60 ± 0.07	5.47–5.73	ND	ND	ND	9.75 ± 1.11
E79K	5.39 ± 0.04	5.30–5.48	ND	ND	ND	1.39 ± 0.06
E79Q	5.53 ± 0.07	5.39–5.67	ND	ND	ND	0.51 ± 0.03
E79D	6.03 ± 0.07	5.85–6.17	ND	ND	ND	0.43 ± 0.02
Y282R	5.64 ± 0.04	5.56–5.72	ND	ND	ND	1.55 ± 0.20
E416C	5.72 ± 0.05	5.63–5.81	7.50 ± 0.02	7.46–7.54	5.3	0.62 ± 0.03
E416C + MTSET	5.55 ± 0.08	5.39–5.70	ND	ND	ND	0.63 ± 0.04
E416K	5.84 ± 0.05	5.75–5.93	7.48 ± 0.02	7.44–7.51	9.2	1.45 ± 0.08
E416Q	5.56 ± 0.06	5.44–5.67	ND	ND	ND	1.04 ± 0.07
E79Q/E416C	5.51 ± 0.06	5.39–5.64	ND	ND	ND	0.75 ± 0.06
E79C/E416Q	5.36 ± 0.03	5.29–5.42	ND	ND	ND	0.42 ± 0.04

that this occurs concurrently with pore opening (16). To investigate conformational rearrangements associated with proton gating in the palm domain, we examined the reactivity toward MTSET of Cys introduced at positions 79 and 416. MTSET is a membrane-impermeable thiol-reactive reagent with a positively charged transferable moiety. E79C and E416C channels were exposed to MTSET at pH 7.0, *i.e.* channels in the desensitized state, or at pH 8.0, *i.e.* channels in the closed state. For these experiments, proton-gated currents were elicited by a change in extracellular pH from 8.0 to 5.0 before and after treatment with MTSET (1 mM). MTSET modifies E79C and E416C channels in a state-dependent manner (Fig. 3, *A*, *D*, and *E*). MTSET treatment at pH 8.0 increased the magnitude of the peak current elicited by extracellular acidification and slowed the current decay during desensitization of E79C channels (Figs. 3 and 4). In contrast, for E416C channels, MTSET treatment at pH 8.0 reduced the magnitude of peak current elicited by extracellular acidification without affecting the rates of desensitization (Fig. 3 and Table 1). Fig. 3*E* shows the fractional activation for E79C channels as a function of the preconditioning pH (*left axis*). At pH 7.4 or below, E79C channels reside in the desensitized state and cannot be activated by extracellular acidification. The normalized relative response to extracellular acidification for E79C channels exposed to MTSET is plotted as a function of the pH of MTSET treatment (Fig. 3*E*, *right axis*). The relative response represents the ratio of the pH-elicited peak current following MTSET treatment to the pH-elicited peak current before treatment. These experiments show that Cys at position 79 reacts with MTSET when channels reside in the closed state, but not in the desensitized state. Similarly, MTSET treatment at pH 7.0 did not alter the response to extracellular acidification of E416C channels (Fig. 3, *A* and *D*). The covalent modification by MTSET of E79C or E416C channels did not change their proton activation curves (Fig. 3, *B* and *C*). Overall, our data indicate that the lower palm domain adopts different conformations at pH 7.0 and 8.0.

The covalent modification by MTSET of E79C channels augments the magnitude of the peak current evoked by extracellular acidification and slows the current decay during desensitization. Mechanistically, the presence of a larger moiety at position 79 may impose a constraint that prevents pore closing during desensitization, affecting simultaneously both the magnitude of the proton-gated currents and the rates of desensitization. We conducted experiments to assess how the length of the transferable moiety attached at position 79 affects proton gating and desensitization. E79C channels were activated by a drop in the extracellular pH from 8.0 to 5.0 before and after treatment with (1-(trimethylammonium)methyl) methanethiosulfonate bromide (MTSMT), MTSET, or (3-(trimethylammonium)propyl) methanethiosulfonate bromide (MTSPT). The transferable moiety of these reagents encompasses a trimethylammonium group and a linker of increasing length (methyl, ethyl, or propyl) (Fig. 4). To estimate the rates of desensitization after modification, channels were exposed to a solution of pH 5.0 for 1 min. The relative response to extracellular acidification was similar for E79C channels covalently modified by MTSMT, MTSET, or MTSPT. E79C channels covalently modified by MTSET desensitize at a slower rate than channels covalently modified by MTSMT or MTSPT, although the values were not statistically different. The results of these experiments indicate that the time course of desensitization of covalently modified E79C channels is slightly dependent on the size of the attached moiety.

Lower Palm Domain Contracts upon Extracellular Acidification—The extracellular vestibule is defined by the most extracellular part of the TMs and the lower palm domain (12, 18). We conducted mutagenesis studies to define the extent of the conformational changes that occur in the palm domain following extracellular acidification. The experiments described above showed that Cys at position 79 reacts with thiol-modifying reagents in the closed state, but not in the desensitized state. Glu-79 is positioned near the subunit-subunit interface in the desensitized state. Essentially, Glu-79 in an ASIC1 subunit is in close proximity to residues in the palm and thumb domains of the neighboring subunit (Fig. 5*A*). We hypothesized that the observed changes in proton gating for covalently modified E79C channels result from a steric effect between the moieties attached at position 79 and residues in the neighboring subunit.

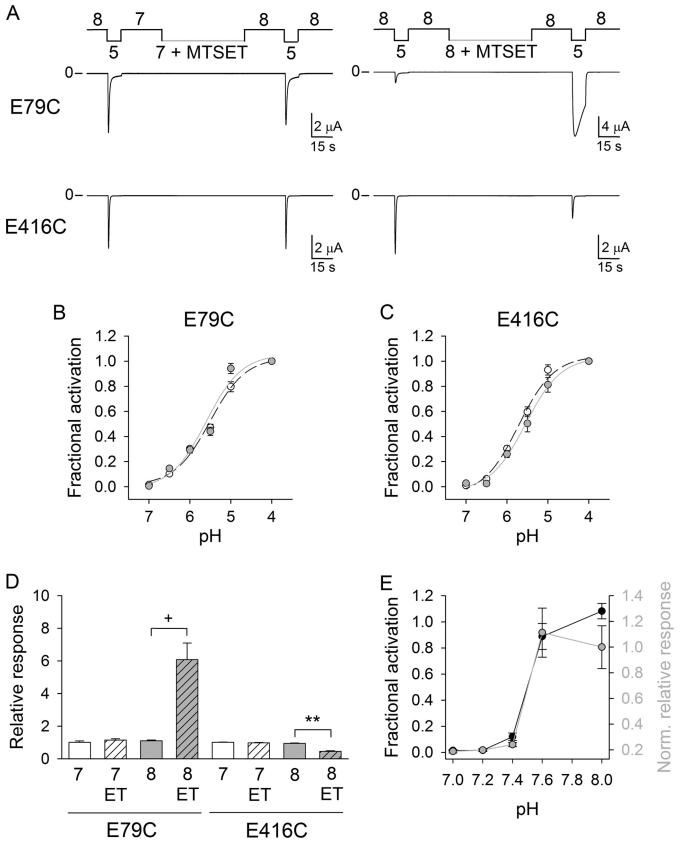

FIGURE 3. **State-dependent reactivity of Cys at positions 79 and 416.** *A*, reactivity toward MTSET of E79C and E416C channels in the closed and desensitized states. Shown are representative recordings of experiments performed with oocytes expressing E79C and E416C channels. Whole-cell currents were elicited by a change in extracellular pH from 8.0 to 5.0 before and after exposure to MTSET (1 mM) at the indicate pH values. Untreated oocytes expressing E79C and E416C channels served as controls. *B* and *C*, proton activation curves for E79C and E416C channels before (*white circles*) and after (*gray circles*) MTSET modification. E79C and E416C channels were covalently modified by MTSET (1 mM) at pH 8.0. Proton-activated currents were elicited by a drop in extracellular pH from 9.0 to solutions of lower pH. Currents were normalized to the signal obtained at pH 4.0 ($n = 8–18$). *D*, chemical modification of E79C and E416C channels in the closed and desensitized states. Whole-cell currents were evoked by a change in extracellular pH from 8.0 to 5.0 as described for *A*. The relative response represents the ratio of the pH-elicited peak current following MTSET (*ET*) treatment (or control) to the pH-elicited peak current before treatment ($n = 10–24$). Statistically significant differences are indicated: **, $p < 0.01$; +, $p < 0.001$ (Kruskal-Wallis test followed by Dunn's multiple comparison test). *E*, state-dependent modification of E79C channels. Shown is the fractional activation as a function of the preconditioning pH (*left axis*, *black circles*). Whole-cell currents were elicited by extracellular acidification to pH 5.0 from a solution of pH 9.0, 8.0, 7.6, 7.4, 7.2, or 7.0. Currents were normalized to the peak current evoked by a drop in extracellular pH from 9.0 to 5.0 ($n = 9–10$). Shown is the chemical modification of E79C as a function of the pH of MTSET treatment (*right axis*, *gray circles*). Whole-cell currents were elicited by a change in extracellular pH from 8.0 to 5.0 before and after exposure to MTSET (1 mM) at pH 7.0, 7.2, 7.4, 7.6, or 8.0. The relative response represents the ratio of the pH-elicited peak current following MTSET treatment to the pH-elicited peak current before treatment ($n = 8–24$). Data were normalized to the mean relative response to extracellular acidification of E79C channels exposed to MTSET at pH 8.0.

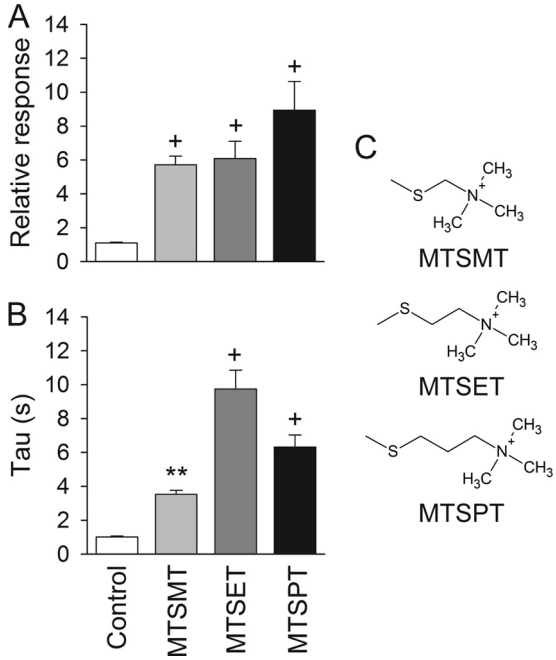

FIGURE 4. **Chemical modification of E79C channels by MTS reagents.** Whole-cell currents were evoked by a change in extracellular pH from 8.0 to 5.0 before and after treatment with MTSMT, MTSET, or MTSPT at pH 8.0. Untreated oocytes expressing E79C served as controls. *A*, relative response to extracellular acidification of covalently modified E79C channels. The relative response represents the ratio of the pH-elicited peak current following MTS reagent treatment (or control) to the pH-elicited peak current before treatment ($n = 10–24$). Statistically significant differences with the control are indicated: +, $p < 0.001$ (Kruskal-Wallis test followed by Dunn's multiple comparison test). *B*, time constants of desensitization of controls and covalently modified E79C channels. Whole-cell currents were fitted to a single exponential function as described under "Experimental Procedures" ($n = 10–24$). Statistically significant differences with the control are indicated: **, $p < 0.01$; +, $p < 0.001$ (Kruskal-Wallis test followed by Dunn's multiple comparison test). *C*, chemical formula of the transferable moiety of MTSMT, MTSET, and MTSPT.

To evaluate intersubunit interactions, we generated E79C constructs with engineered Ala substitutions at positions neighboring residue 79. Glu-79 is in close proximity to Gln-278, Leu-280, Tyr-282, Met-363, Arg-369, Glu-416, and Ile-418 in the neighboring subunit in the desensitized state (Fig. 5*A*). Proton-gated currents were elicited by a change in extracellular pH from 8.0 to 5.0 before and after MTSET treatment at pH 8.0 (closed state) (Fig. 5). The relative response to extracellular acidification was significantly increased for E79C/L280A, E79C/Y282A, and E79C/I418A channels compared with controls (E79C). Remarkably, proton-gated currents were only occasionally observed in oocytes expressing E79C/Y282A channels before MTSET treatment. The covalent modification of this mutant increased proton-gated currents by >150-fold. This suggests that the bulky moiety of MTSET attached at position 79 facilitates pore opening in response to extracellular acidification (Fig. 5). MTSET-modified E79C/L280A, E79C/Y282A, and E79C/E416Q channels desensitized faster than controls. This indicates that Ala substitutions at positions 280 and 282 disturb steric interactions with the moiety attached at position 79 (Fig. 5*D*). E79C/E416C and E79C/E416A channels were not activated by extracellular acidification before or after MTSET exposure (data not shown). Taken together, our data suggest that extracellular acidification brings Glu-79 closer to residues in the palm and thumb domains of the adjacent subunit.

Intersubunit Salt Bridges Alter Transitions between the Desensitized and Closed States—To probe further intersubunit interactions in the lower palm domain, we engineered Arg substitutions at positions 278, 280, and 282 in ASIC1a. The ration-

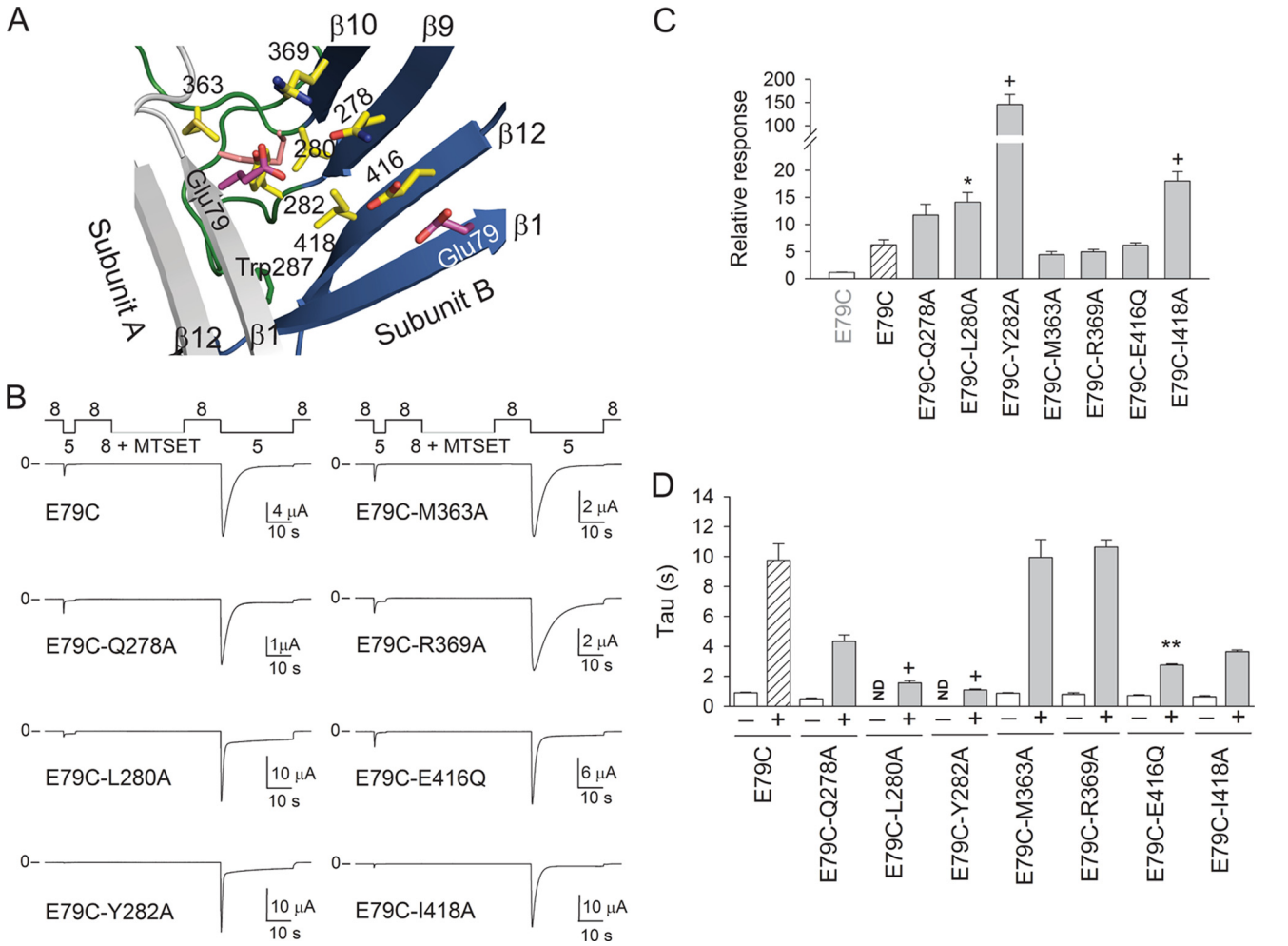

FIGURE 5. **Ala substitutions in the palm and thumb domains alter E79C proton gating.** *A*, structural model of ASIC1 in the desensitized state illustrating residues neighboring Glu-79. Subunit A is shown in *gray*, and subunit B is *multicolored*. *B*, representative recordings of experiments performed with oocytes expressing E79C (control) and double mutant channels exposed to MTSET at pH 8.0. Whole-cell currents were evoked by a change in extracellular pH from 8.0 to 5.0. Note the deficient response of non-modified E79C/Y282A channels to extracellular acidification. *C*, relative response to extracellular acidification of covalently modified E79C and double mutant channels. The relative response represents the ratio of the pH-elicited peak current following MTSET treatment to the pH-elicited peak current before treatment ($n = 10–26$). Statistically significant differences between covalently modified double mutant channels and covalently modified E79C channels are indicated: *, $p < 0.05$; +, $p < 0.001$ (Kruskal-Wallis test followed by Dunn's multiple comparison test). *D*, time constants of desensitization of ASIC1a mutant channels. Whole-cell currents were fitted to a single exponential function as described under "Experimental Procedures." Statistically significant differences between covalently modified double mutant channels and covalently modified E79C channels are indicated: **, $p < 0.01$; +, $p < 0.001$ (Kruskal-Wallis test followed by Dunn's multiple comparison test). *ND*, not determined.

ale was to engineer favorable electrostatic interactions between Glu-79 and residues in neighboring subunits and to assess their impact on proton gating. Representative experiments performed with Q278R and L280R channels are shown in Fig. 6. Although Q278R and L280R channels underwent activation and desensitization following extracellular acidification similarly to controls (C70L), the magnitude of the peak current evoked by extracellular acidification was significantly reduced upon successive stimulations (Fig. 6*A*). Remarkably, the rates of desensitization of Q278R and L280R channels were not different from those of controls. In contrast, Y282R channels underwent activation and desensitization in response to extracellular acidification similarly to controls. The pH_{50} for Y282R channels was shifted toward more acidic values, likewise channels bearing a Cys, Lys, or Gln mutation at position 79 (Fig. 7). These results suggest that electrostatic interactions between Glu-79 and engineered Arg in the adjacent subunit alter proton-mediated conformational changes.

DISCUSSION

Here, we report that Glu-79 and Glu-416 in the lower palm domain cooperatively contribute to ASIC1a proton gating. Non-conservative substitutions at these positions shifted the pH_{50} toward more acidic values but did not impair channel function. Substitutions at positions 79 and 416 affected activation, but not steady-state desensitization. A conservative Asp substitution at position 79 shifted the pH_{50} toward more acidic values, although to a lesser extent than for channels bearing non-conservative mutations at this position. These findings suggest that Glu-79 and Glu-416 are part of the proton-sensing machinery in ASIC1a. Indeed, based on the close proximity of Glu-79 and Glu-416 in the cASIC1 structure, it was proposed that at least one of the carboxyl groups in this pair is protonated in the desensitized state (12). Recently, Dawson *et al.* (19) reported that Glu-416 and Glu-79 might be involved in cation and water coordination. Our double mutant cycle analysis sup-

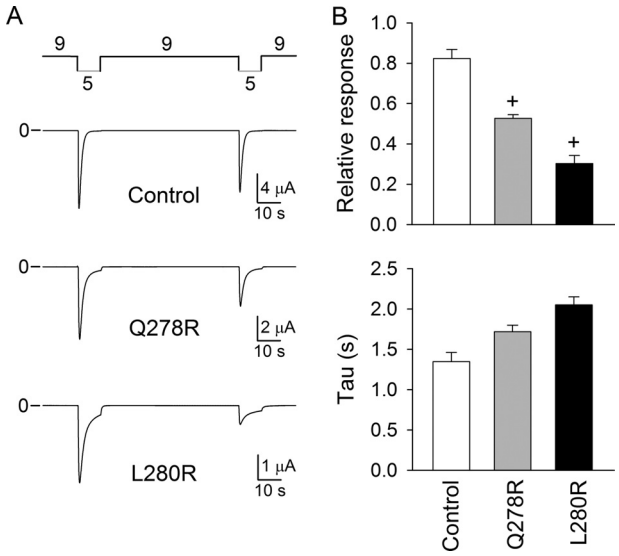

FIGURE 6. **Arg substitutions in the palm domain reduce the response to successive stimulations.** *A*, representative recordings of experiments performed with oocytes expressing control (C70L) and mutant channels. *B*, *upper panel*, Q278R and L280R channels show reduced responses to successive stimulations. The relative response represents the ratio of the pH-elicited peak currents from two consecutive stimulations ($n = 18–22$). Statistically significant differences with the control are indicated: +, $p < 0.001$ (Kruskal-Wallis test followed by Dunn's multiple comparison test). Oocytes expressing C70L channels served as controls. *Lower panel*, time constants of desensitization of ASIC1a mutant channels. Whole-cell currents were fitted to a single exponential function as described under "Experimental Procedures" ($n = 17–23$).

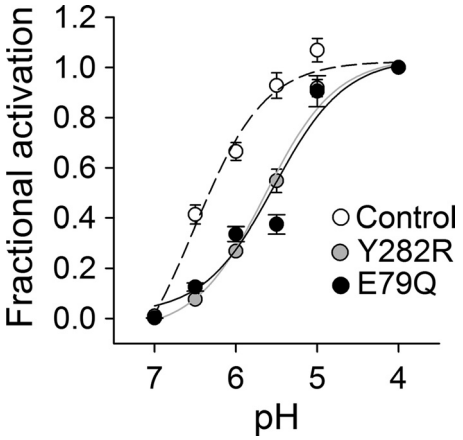

FIGURE 7. **Arg substitution at position 282 shifts proton apparent affinity.** Shown are proton activation curves for control and mutant channels. Proton-activated currents were elicited by a drop in extracellular pH from 9.0 to solutions of lower pH. Currents were normalized to the signal obtained at pH 4.0 ($n = 10–25$).

ports a functional interaction between Glu-79 and Glu-416. The results of our studies indicate that Glu-79 and Glu-416 facilitate pore opening in response to extracellular acidification, although they are not essential for proton-dependent gating.

Glu-79 and nearby residues are critical for ASIC3 acid-induced desensitization (22). Mutating Glu-79 to Ala in ASIC3 shifts steady-state desensitization dramatically toward more basic values and speeds up desensitization rates, without noticeable effects on activation (22). In contrast, ASIC1a with engineered mutations at position 79 shows an important shift in the apparent proton affinity toward more acidic values, a modest change in the apparent proton affinity for steady-state desensitization, and a faster desensitization (this study and Ref. 25). We hypothesize that the different outcome that substitutions at this position have on the activation and desensitization of ASIC1a and ASIC3 might be due to structural and functional differences between these isoforms.

Our functional studies, as well as information obtained from the cASIC1 structure, suggest that at least one of the carboxyl groups in the Glu-79/Glu-416 pair becomes protonated following extracellular acidification. Because extracellular acidification likely triggers a reorganization of the extracellular region, protonable sites might be accessible in the closed state but buried in the desensitized state. To explore this possibility, we conducted studies of accessibility with MTS reagents on channels with an engineered Cys substitution at position 79 or 416. MTSET reacted with Cys residues introduced at positions 79 and 416 at pH 8.0, *i.e.* channels in the closed state, but not at pH 7.0, *i.e.* channels in the desensitized state. Likewise, Cys at position 79 in ASIC3 can be modified in a state-dependent manner by the negatively charged thiol-reactive reagent (2-sulfonatoethyl) methanethiosulfonate sodium salt (MTSES) (22). Our studies indicate that Glu-79 and Glu-416 are accessible for covalent modification in the closed state but are buried in the desensitized state.

The covalent modification of Cys at position 79 increased the magnitude of the peak current evoked by extracellular acidification and slowed the current decay during desensitization, whereas the modification of Cys at position 416 reduced the peak current without a noticeable effect on desensitization. Notably, the effects of the covalent modification of Cys at position 79 or 416 became evident only during activation following extracellular acidification, suggesting regional proton-dependent conformational rearrangements. β1 and β12 are directly linked to TM1 and TM2, respectively. The introduction of bulky moieties in β1 and β12 is likely to have an impact on the dynamics of pore opening and closing events that occur upon extracellular acidification. TM2 defines the permeation pathway, whereas TM1 resides in the periphery of the pore. Our results show that moieties attached at position 416 in β12 constrain motions associated with pore opening, whereas moieties attached at position 79 impact conformational rearrangements associated with pore closing during desensitization. In good agreement with our studies, Coric *et al.* (26) identified a cluster of three residues in a loop distal to β1 (Ser-83–Gln-84–Leu-85 in rat and Pro-83–Leu-84–Met-85 in fish) that accounts for the faster desensitization rate of fish ASIC1 compared with rat ASIC1a. Recently, Springauf *et al.* (27) reported that spontaneous cross-linking of engineered Cys introduced in the β1-β2 and β11-β12 linkers traps ASIC1a in an unresponsive closed state. Overall, these studies emphasize the role of the palm domain in proton gating and desensitization of ASIC1a.

Glu-79 in a subunit is situated in close proximity to residues in the palm and thumb domains of the adjacent subunit in the desensitized state. Our data suggest that the transferable moiety attached at position 79 becomes closer to residues in the palm and thumb domains of the neighboring subunit in response to extracellular acidification. Remarkably, the covalent modification by MTSET of E79C/Y282A channels increased proton-gated current by almost 150-fold. Proton-gated currents were barely observed in oocytes expressing this

mutant before MTSET treatment. Tyr-282 does not seem to be essential for proton gating because Y282R channels are functional. We hypothesize that the absence of a response to extracellular acidification of E79C/Y282A channels results from deficient subunit-subunit interactions. Our studies indicate that the distance between Glu-79 and neighboring residues in the palm and thumb domains varies as channels transition between the closed, open, and desensitized states. The atomic structure of ASIC1 in the closed state is not currently available. Based on the structural data gathered from the solved atomic structures of psalmotoxin-cASIC1 complexes at low and high pH values, Baconguis and Gouaux (18) proposed that the extracellular vestibule resides in an expanded conformation at high pH and that it adopts a contracted conformation following extracellular acidification. Our functional studies are consistent with this model.

Arg substitutions at positions 278 and 280 reduced the magnitude of the peak current after successive acidic stimulations, without any noticeable effect on the rates of desensitization. These mutations seem to hold the channel in an unresponsive state, most likely by affecting the recovery from desensitization. We hypothesize that electrostatic interactions between Glu-79 and engineered Arg in the adjacent subunit occur after extracellular acidification. In the resting state, these residues are distant and unable to interact. Interestingly, some channels bearing Cys at position 79 and Ala mutations in the palm or thumb domains, as well as Q278R and L280R channels, do not desensitize completely after extracellular acidification. Mutations at these positions constrain conformational changes associated with pore closing during desensitization, suggesting that palm-thumb domain interactions have a critical role in this process.

ASICs have been proposed as potential therapeutic targets to treat pain, psychiatric disorders, and neurodegenerative diseases (8, 28). Yu *et al.* (29) identified 2-guanidine-4-methylquinazoline (GMQ) as a non-proton ligand for ASIC3. They proposed that Glu-423 and Glu-79 in the palm domain of ASIC3 serve as ligand sensors for GMQ. A recent study that evaluated the underlying mechanisms of GMQ in different ASIC isoforms concluded that Glu-79 is not directly involved in the binding interaction (25). Although the molecular mechanism of action of GMQ remains unclear at the present, both studies showed that substitutions at position 79 of ASIC3 prevent activation by GMQ. Because the lower palm domain experiences significant structural rearrangements in response to extracellular acidification, residues in this region and particularly those lining the extracellular vestibule can serve as potential targets for small modulatory compounds.

In summary, our data indicate that the lower palm domain contracts upon extracellular acidification. The covalent modification of Cys residues introduced in β1 and β12 impacts antagonistically proton gating and desensitization. Our results suggest that conformational rearrangements in the lower palm domain of ASIC1a mediate pore opening and closing events in response to extracellular acidification.

Acknowledgments—We thank Ossama Kashlan and Aram Krauson for critical reading of the manuscript.

REFERENCES

1. Wemmie, J. A., Chen, J., Askwith, C. C., Hruska-Hageman, A. M., Price, M. P., Nolan, B. C., Yoder, P. G., Lamani, E., Hoshi, T., Freeman, J. H., Jr., and Welsh, M. J. (2002) The acid-activated ion channel ASIC contributes to synaptic plasticity, learning, and memory. *Neuron* **34,** 463–477
2. Wemmie, J. A., Coryell, M. W., Askwith, C. C., Lamani, E., Leonard, A. S., Sigmund, C. D., and Welsh, M. J. (2004) Overexpression of acid-sensing ion channel 1a in transgenic mice increases acquired fear-related behavior. *Proc. Natl. Acad. Sci. U.S.A.* **101,** 3621–3626
3. Price, M. P., Lewin, G. R., McIlwrath, S. L., Cheng, C., Xie, J., Heppenstall, P. A., Stucky, C. L., Mannsfeldt, A. G., Brennan, T. J., Drummond, H. A., Qiao, J., Benson, C. J., Tarr, D. E., Hrstka, R. F., Yang, B., Williamson, R. A., and Welsh, M. J. (2000) The mammalian sodium channel BNC1 is required for normal touch sensation. *Nature* **407,** 1007–1011
4. Deval, E., Gasull, X., Noël, J., Salinas, M., Baron, A., Diochot, S., and Lingueglia, E. (2010) Acid-sensing ion channels (ASICs): pharmacology and implication in pain. *Pharmacol. Ther.* **128,** 549–558
5. Lingueglia, E. (2007) Acid-sensing ion channels in sensory perception. *J. Biol. Chem.* **282,** 17325–17329
6. Lu, Y., Ma, X., Sabharwal, R., Snitsarev, V., Morgan, D., Rahmouni, K., Drummond, H. A., Whiteis, C. A., Costa, V., Price, M., Benson, C., Welsh, M. J., Chapleau, M. W., and Abboud, F. M. (2009) The ion channel ASIC2 is required for baroreceptor and autonomic control of the circulation. *Neuron* **64,** 885–897
7. Sherwood, T. W., Frey, E. N., and Askwith, C. C. (2012) Structure and activity of the acid-sensing ion channels. *Am. J. Physiol. Cell Physiol.* **303,** C699–C710
8. Wemmie, J. A., Price, M. P., and Welsh, M. J. (2006) Acid-sensing ion channels: advances, questions and therapeutic opportunities. *Trends Neurosci.* **29,** 578–586
9. Benson, C. J., Xie, J., Wemmie, J. A., Price, M. P., Henss, J. M., Welsh, M. J., and Snyder, P. M. (2002) Heteromultimers of DEG/ENaC subunits form H^+-gated channels in mouse sensory neurons. *Proc. Natl. Acad. Sci. U.S.A.* **99,** 2338–2343
10. Gautam, M., and Benson, C. J. (2012) Acid-sensing ion channels (ASICs) in mouse skeletal muscle afferents are heteromers composed of ASIC1a, ASIC2, and ASIC3 subunits. *FASEB J.* DOI 10.1096/fj.12-220400
11. Kellenberger, S., and Schild, L. (2002) Epithelial sodium channel/degenerin family of ion channels: a variety of functions for a shared structure. *Physiol. Rev.* **82,** 735–767
12. Jasti, J., Furukawa, H., Gonzales, E. B., and Gouaux, E. (2007) Structure of acid-sensing ion channel 1 at 1.9 Å resolution and low pH. *Nature* **449,** 316–323
13. Li, T., Yang, Y., and Canessa, C. M. (2009) Interaction of the aromatics Tyr-72/Trp-288 in the interface of the extracellular and transmembrane domains is essential for proton gating of acid-sensing ion channels. *J. Biol. Chem.* **284,** 4689–4694
14. Paukert, M., Chen, X., Polleichtner, G., Schindelin, H., and Gründer, S. (2008) Candidate amino acids involved in H^+ gating of acid-sensing ion channel 1a. *J. Biol. Chem.* **283,** 572–581
15. Liechti, L. A., Bernèche, S., Bargeton, B., Iwaszkiewicz, J., Roy, S., Michielin, O., and Kellenberger, S. (2010) A combined computational and functional approach identifies new residues involved in pH-dependent gating of ASIC1a. *J. Biol. Chem.* **285,** 16315–16329
16. Passero, C. J., Okumura, S., and Carattino, M. D. (2009) Conformational changes associated with proton-dependent gating of ASIC1a. *J. Biol. Chem.* **284,** 36473–36481
17. Shi, S., Carattino, M. D., and Kleyman, T. R. (2012) Role of the wrist domain in the response of the epithelial sodium channel to external stimuli. *J. Biol. Chem.* **287,** 44027–44035
18. Baconguis, I., and Gouaux, E. (2012) Structural plasticity and dynamic selectivity of acid-sensing ion channel-spider toxin complexes. *Nature* **489,** 400–405
19. Dawson, R. J., Benz, J., Stohler, P., Tetaz, T., Joseph, C., Huber, S., Schmid, G., Hügin, D., Pflimlin, P., Trube, G., Rudolph, M. G., Hennig, M., and Ruf, A. (2012) Structure of the acid-sensing ion channel 1 in complex with the gating modifier Psalmotoxin 1. *Nat. Commun.* **3,** 936

20. Tolino, L. A., Okumura, S., Kashlan, O. B., and Carattino, M. D. (2011) Insights into the mechanism of pore opening of acid-sensing ion channel 1a. *J. Biol. Chem.* **286,** 16297–16307
21. Chen, X., and Gründer, S. (2007) Permeating protons contribute to tachyphylaxis of the acid-sensing ion channel (ASIC) 1a. *J. Physiol.* **579,** 657–670
22. Cushman, K. A., Marsh-Haffner, J., Adelman, J. P., and McCleskey, E. W. (2007) A conformation change in the extracellular domain that accompanies desensitization of acid-sensing ion channel (ASIC) 3. *J. Gen. Physiol.* **129,** 345–350
23. Hidalgo, P., and MacKinnon, R. (1995) Revealing the architecture of a K^+ channel pore through mutant cycles with a peptide inhibitor. *Science* **268,** 307–310
24. Horovitz, A., and Fersht, A. R. (1990) Strategy for analysing the cooperativity of intramolecular interactions in peptides and proteins. *J. Mol. Biol.* **214,** 613–617
25. Alijevic, O., and Kellenberger, S. (2012) Subtype-specific modulation of acid-sensing ion channel (ASIC) function by 2-guanidine-4-methylquinazoline. *J. Biol. Chem.* **287,** 36059–36070
26. Coric, T., Zhang, P., Todorovic, N., and Canessa, C. M. (2003) The extracellular domain determines the kinetics of desensitization in acid-sensitive ion channel 1. *J. Biol. Chem.* **278,** 45240–45247
27. Springauf, A., Bresenitz, P., and Gründer, S. (2011) The interaction between two extracellular linker regions controls sustained opening of acid-sensing ion channel 1. *J. Biol. Chem.* **286,** 24374–24384
28. Qadri, Y. J., Rooj, A. K., and Fuller, C. M. (2012) ENaCs and ASICs as therapeutic targets. *Am. J. Physiol. Cell Physiol.* **302,** C943–C965
29. Yu, Y., Chen, Z., Li, W. G., Cao, H., Feng, E. G., Yu, F., Liu, H., Jiang, H., and Xu, T. L. (2010) A nonproton ligand sensor in the acid-sensing ion channel. *Neuron* **68,** 61–72